# Surface wave interaction with rigid plates lying on water

Richard Porter

*School of Mathematics, University of Bristol, Bristol, BS8 1TW, UK*

**Abstract**

In this paper, a variety of problems concerned with the interaction of water waves with fixed horizontal plates lying on the surface of a fluid are investigated.

Firstly, solutions are presented to the problem of the scattering of incident waves by: (i) infinitely-long plates of constant finite width (often referred to as the two-dimensional 'finite dock problem') and (ii) finite plates which are either rectangular or parallelogram-shaped. Secondly, hydrodynamic coefficients due to forced motions of plates are also considered. Finally, eigenvalue problems associated with free oscillations of the surface in long channels of uniform width and finite rectangular holes in an otherwise infinite rigid plate covering the surface are considered.

A common method of solution is applied to all problems which involves using Fourier transforms to derive integral equations for unknown potentials over finite regions of space occupied by either plates or the free surface. Integral equations are converted, using the Galerkin method, into second-kind infinite systems of algebraic equations. In each problem numerical approximations to the solutions are found to converge rapidly with increasing truncation size of the infinite system making this approach both numerically efficient and accurate. Some comparisons with existing results are made, and new results for finite plates are demonstrated.

*Keywords:* Finite dock, ice fishing hole, Fourier transform solution, integral equations.

## 1. Introduction

The reflection and transmission of surface gravity waves by a rigid plate or 'dock' on the surface of a fluid is a classical problem in the study of linearised water waves. For example, when the plate covers the half-plane – the so-called semi-infinite dock problem – an explicit expression for the reflection coefficient can be found using the Wiener-Hopf technique ([1], [2], [3] for example). For a plate that is infinitely-long in one direction and of uniform constant width in the perpendicular direction – the so-called 'finite dock problem' – exact solutions are no longer possible and various techniques have been employed all leading to approximations of the reflection and transmission

*Email address:* richard.porter@bristol.ac.uk (Richard Porter)

coefficients. See, for example, [3], [4] who base solutions on short wave asymptotic approximations and [5], [6] who use domain decomposition in finite water depth combined with a modified residue calculus technique, and references therein.

We start this paper by revisiting the finite dock problem in fluid of infinite depth. The detailed changes required for constant finite depth are easily implemented following the methods we employ (or consult [7]) but are omitted here in order to retain simplicity. Owing to the geometry, the problem under consideration is quasi two-dimensional, the obliqueness of the plane monochromatic incident waves implying that the governing equation is transformed from Laplace's to the modified Helmholtz equation. Investigation of the oblique finite dock problem allows us to establish the basic method of solution and assess the performance of the numerical method against known results. The solution is derived by initially using Fourier transforms to formulate an integral equation for the unknown potential under the plate. This is expanded in a series of Legendre polynomials and the integral equation is thus transformed into a second-kind infinite system of equations for the coefficients in the expansion. This is shown to involve matrix elements which are easy to compute accurately. Furthermore, results show that the system of equations converges rapidly with increasing truncation size. This general approach forms the basis of recent work on similar problems involving submerged plates by [7] and has similarities to work by [8] for radiation of internal gravity waves by discs oscillating in a stratified fluid and [9] for scattering of surface waves by cracks in elastic solids.

The application of the approach adopted here appears new. Unlike modified residue calculus methods (e.g. [6]) the method can be applied in water of infinite depth and finite depth. For finite depth, knowledge of the all roots of dispersion relations in the complex plane is not necessary – this is not an issue in the problems illustrated here, but could be if the method were applied to problems with more complex boundary conditions such as those involving elastic or porous plates. The general approach is restricted to those problems for which taking Fourier transforms is possible but has the advantage over approaches based on Green's functions of bypassing technical difficulties with singularities (see [10] for example). From a practical perspective the numerical implementation of the solution is very simple and for low frequency/short plates results in rapidly convergent numerical solutions requiring little computational effort. For high frequency/longer plates, the numerical method requires more effort as it aims to reconstruct properties of the field along the plate in a finite series of functions. In these cases, methods which incorporate the explicit solutions to the solution of a semi-infinite dock (see [6]) have an advantage.

One major factor in adopting this method of solution is that it lends itself to being extended to a

more general class of problem and this is pursued throughout the remainder of the paper. Thus, we continue the paper by considering the three-dimensional scattering of waves by a thin finite plate of arbitrary shape fixed in the free surface. Apart from where the plate is circular (when separation of variables can be used, e.g. [11]) there appears to be little work on this problem. For floating elastic plates of arbitrary planform [12], [13] have derived a semi-analytical approach based on Green's function combined with a boundary element discretisation. For certain geometrically simple shapes of plate shown in this paper (rectangles, circles, parallelograms) the Fourier transform approach avoids this level of complication.

To extend the approach used for the finite dock problem to this new problem we simply implement a double Fourier transform to develop integral equations which retain the same overall structure of the solution as before. The reduction to an infinite algebraic system of equations now involves terms which are more computationally intensive, being defined by double integrals over Fourier space as opposed to single integrals previously. However, since the numerical method converges rapidly with increasing truncation size, numerical solutions remain quick to compute. Another advantage of the method described in the paper is that solutions are easily adapted for parallelogram-shaped plates.

In the last main section, we consider a set of problems in which the regions occupied by the free surface and the plate are interchanged. Thus the fluid is now bounded above by an infinite rigid lid within which a finite hole is cut to leave the fluid exposed to the atmosphere. The problem is one of determining the natural sloshing modes in this so-called 'ice fishing problem'; see [14]. Again, this is a problem with a long history particularly in two dimensions; papers of particular note in this respect include [15], [16], [17].

## 2. The oblique-incidence finite-dock problem

Cartesian coordinates are used with $z = 0$ coinciding with the mean free surface and the fluid extending into $z < 0$. A rigid horizontal plate is placed on the surface, $z = 0$, and extends uniformly in the $y$ direction and from $x = -a$ to $x = a$ in the $x$-direction. Assuming time-harmonic incident waves of angular frequency $\omega$ making an angle $\theta_0 \in (-\frac{1}{2}\pi, \frac{1}{2}\pi)$ with respect to the positive $x$ direction, the velocity field can be found from the gradients of $\Re\{\Phi(x, y, z)\mathrm{e}^{-\mathrm{i}\omega t}\}$ where the velocity potential $\Phi(x, y, z)$ satisfies

$$\nabla^2\Phi = 0, \qquad z < 0 \tag{1}$$

the linearised free surface condition

$$\left(\frac{\partial}{\partial z} - K\right)\Phi = 0, \qquad z = 0 \tag{2}$$

where $K = \omega^2/g$ and $g = 9.81\text{ms}^{-2}$ is gravity, and

$$|\nabla\Phi| \to 0, \qquad z \to -\infty. \tag{3}$$

The incident wave is represented by the potential

$$\Phi_{inc} = \mathrm{e}^{\mathrm{i}\alpha_0 x}\mathrm{e}^{\mathrm{i}\beta_0 y}\mathrm{e}^{Kz} \tag{4}$$

where $\alpha_0 = K\cos\theta_0$, $\beta_0 = K\sin\theta_0$.

In this problem where the plate in the surface is uniform in $y$, the total potential responds with the same $y$-variation imposed by the incident wave allowing us to write $\Phi(x, y, z) = \phi(x, z)\mathrm{e}^{\mathrm{i}\beta_0 y}$. Then the reduced two-dimensional potential $\phi(x, z)$ satisfies

$$(\nabla^2 - \beta_0^2)\phi(x, z) = 0, \qquad z < 0, \tag{5}$$

with (2) and (3) applying to $\phi(x, z)$. The zero-velocity condition to be applied on the plate is

$$\phi_z(x, 0) = 0, \qquad |x| < a \tag{6}$$

and at the ends of the plate (as $x$ approaches $\pm a$) the potential should be bounded, though the velocity is logarithmically singular (see [18] or [15]). Finally radiation conditions are required as $|x| \to \infty$. We write

$$\phi(x, z) \sim \begin{cases} \phi_{inc}(x, z) + R\phi_{inc}(-x, z), & x \to -\infty \\ T\phi_{inc}(x, z), & x \to \infty \end{cases} \tag{7}$$

where $R$ and $T$ are the complex reflection and transmission coefficients and $\phi_{inc}(x, z) = \mathrm{e}^{\mathrm{i}\alpha_0 x}\mathrm{e}^{Kz}$. The Fourier transform of the scattered part of the potential is defined by

$$\overline{\phi}(\alpha, z) = \int_{-\infty}^{\infty} (\phi(x, z) - \phi_{inc}(x, z))\mathrm{e}^{-\mathrm{i}\alpha x}\, dx. \tag{8}$$

Applying (5) to (8) gives

$$\left(\frac{d^2}{dz^2} - k_0^2\right)\overline{\phi}(\alpha, z) = 0, \qquad z < 0 \tag{9}$$

where $k_0^2 = \alpha^2 + \beta_0^2$ with $\overline{\phi}(\alpha, z) \to 0$ as $z \to -\infty$ and

$$\left(\frac{d}{dz} - K\right)\overline{\phi}(\alpha, 0) = -K\overline{P}(\alpha), \qquad \text{where} \quad \overline{P}(\alpha) = \int_{-a}^{a} \phi(x, 0)\mathrm{e}^{-\mathrm{i}\alpha x}\, dx \tag{10}$$

after (6) and the free surface condition have been used. Solving (9) and (10) gives

$$\overline{\phi}(\alpha, z) = \frac{K\overline{P}(\alpha)\mathrm{e}^{k_0 z}}{K - k_0} \tag{11}$$

and taking inverse transforms gives

$$\phi(x, z) = \phi_{inc}(x, z) + \frac{K}{2\pi}\int_{-\infty}^{\infty} \frac{\mathrm{e}^{k_0 z}\mathrm{e}^{\mathrm{i}\alpha x}}{K - k_0}\overline{P}(\alpha)\, d\alpha. \tag{12}$$

There are poles on the real $\alpha$-axis at $\alpha = \pm\alpha_0$ where $k_0 = K$. The contour of integration is taken to pass over the pole at $-\alpha_0$ and under the pole at $\alpha_0$ in order to satisy the radiation condition that $\phi - \phi_{inc}$ is outgoing. An alternative approach it to assign a small positive imaginary part to the frequency, $\omega$, which is eventually set to zero. This manifests itself by moving poles at $\alpha = \pm\alpha_0$, above and below the real $\alpha$-axis respectively, allowing the contour of integration to sit on the real $\alpha$-axis.

Under either approach, as we let $x \to \pm\infty$ in (12) we can deform the contour respectively into the upper-half or lower-half $\alpha$-plane, capturing the residues at $\pm\alpha_0$ resulting in

$$T = 1 - \mathrm{i}\mu\overline{P}(\alpha_0), \qquad \text{and} \qquad R = -\mathrm{i}\mu\overline{P}(-\alpha_0) \tag{13}$$

when (7) is used along with the abbreviation $\mu = K^2/\alpha_0 \equiv K\sec\theta_0$. As $\theta_0$ approaches $\frac{1}{2}\pi$, $\mu \to \infty$ and simultaneously $\overline{P}(\pm\alpha_0) \to 0$ in order to balance the integral (12) in with the other bounded terms due to the two poles $\pm\alpha_0$ both approaching the origin. Numerically $T \to 0$ and $R \to -1$ as $\theta_0 \to \frac{1}{2}\pi$. With some effort, this can also be deduced from an arduous asymptotic analysis of the numerical system of equations formulated in the next subsection.

Since (6) has already been applied in the transform solution, we may now simply set $z = 0$ in (6) to obtain

$$\phi(x, 0) + (\mathcal{K}_0\phi)(x) = \mathrm{e}^{\mathrm{i}\alpha_0 x} \tag{14}$$

where

$$(\mathcal{K}_0\phi)(x) = \frac{K}{2\pi}\int_{-\infty}^{\infty} \frac{\mathrm{e}^{\mathrm{i}\alpha x}}{k_0 - K}\int_{-a}^{a} \phi(x', 0)\mathrm{e}^{-\mathrm{i}\alpha x'}\, dx'\, d\alpha. \tag{15}$$

Thus $\phi(x, 0)$ is determined for $|x| < a$ from (14), a second-kind integral equation when restricted to $|x| < a$. Subsequently, $\phi(x, 0)$ can be used in (10) to determine $R$ and $T$ from (13). Also, (14) can be used to represent $\phi(x, 0)$, and hence the free surface, for $|x| > a$, in terms of those values determined for $|x| < a$.

We remark here that an alternative approach (see [7]) is possible in which the integral in (12) is expressed as a real Cauchy principal-value integral plus contributions from each of the two poles at $\alpha = \pm\alpha_0$, being one half of the residues calculated in (13). Such an approach leads to real

integral equations in which $R$ and $T$ can ultimately be found from a scattering matrix formulation involving real inner products. The structure of this formulation of the problem allows the energy relation $|R|^2 + |T|^2 = 1$ to be shown to be satisfied exactly, whatever approximation is made to the solution of the integral equation. However, it is not an approach which is readily generalised to later problems of interest so we have not pursued it here. The rearrangement just described is manifested in the solution below as a reorganisation of complex systems of equations into real systems of equations and thus the satisfaction of $|R|^2 + |T|^2 = 1$ is also guaranteed by our solution approach and confirmed numerically to machine precision.

*2.1. Solution of integral equations*

The unknown in (14) is expanded in terms of a set of prescribed functions,

$$\phi(x,0) = \sum_{n=0}^{\infty} a_n p_n(x/a), \qquad |x| \le a \tag{16}$$

with unknown complex-valued coefficients $a_n$ where

$$p_n(t) = \tfrac{1}{2}\mathrm{e}^{\mathrm{i}n\pi/2} P_n(t) \tag{17}$$

and $P_n$ are orthogonal Legendre polynomials. Other choices of expansion function are possible, but this choice arguably provides the maximum simplification to subsequent results. Of particular note is the identity

$$\int_{-1}^{1} p_n(t)\mathrm{e}^{-\mathrm{i}\sigma t}\, dt = j_n(\sigma) \tag{18}$$

(see [19, eqn. 10.1.14]) where $j_n$ is a spherical Bessel function and $j_n(-\sigma) = (-1)^n j_n(\sigma)$ with $j_n(0) = \delta_{n0}$. For example,

$$j_0(\sigma) = \frac{\sin\sigma}{\sigma}, \qquad j_1(\sigma) = \frac{\sin\sigma - \sigma\cos\sigma}{\sigma^2} \tag{19}$$

whilst $j_{n+1}(\sigma) = (2n+1)j_n(\sigma)/\sigma - j_{n-1}(\sigma)$. We also note the relation

$$j_n(\sigma) = \sqrt{\frac{\pi}{2\sigma}} J_{n+1/2}(\sigma) \tag{20}$$

to the standard Bessel function.

The expansion (16) is substituted into (14) which is multiplied through by $p_m^*(x/a)$ and integrated over $-a < x < a$. This procedure results in the following infinite system of equations for the unknown coefficients $a_n$:

$$\frac{a_m}{2(2m+1)} + \sum_{n=0}^{\infty} a_n K_{m,n} = j_m(\alpha_0 a), \qquad m = 0, 1, 2, \ldots \tag{21}$$

where

$$K_{m,n} = \frac{Ka}{2\pi}\int_{-\infty}^{\infty} \frac{j_n(\alpha a) j_m(\alpha a)}{k_0 - K}\, d\alpha. \tag{22}$$

In deriving this system of equations we have used the orthogonality relation satisfied by the Legendre polynomials (e.g. [20, §7.221(2)]).

Noting from (22) that $K_{mn} = 0$ if $m + n$ is odd implies a decoupling of (21) into its symmetric and antisymmetric parts for $a_{2n}$ and $a_{2n+1}$. Hence, (21) is most efficiently expressed as

$$\frac{a_{2m+\nu}}{2(4m+1+2\nu)} + \sum_{n=0}^{\infty} a_{2n+\nu} K_{2m+\nu,2n+\nu} = j_{2m+\nu}(\alpha_0 a), \qquad m = 0, 1, 2, \ldots \tag{23}$$

for $\nu = 0, 1$ where now

$$K_{2m+\nu,2n+\nu} = \frac{Ka}{\pi}\int_0^{\infty} \frac{j_{2n+\nu}(\alpha a) j_{2m+\nu}(\alpha a)}{k_0 - K}\, d\alpha \tag{24}$$

is symmetric with respect to $m$ and $n$. For numerical purposes we now deform the contour of integration (or let the imaginary part of $K$ tend to zero) so that (24) may be written

$$K_{2m+\nu,2n+\nu} = \frac{Ka}{\pi}\fint_0^{\infty} \frac{j_{2n+\nu}(\alpha a) j_{2m+\nu}(\alpha a)}{k_0 - K}\, d\alpha + \mathrm{i}\mu a j_{2n+\nu}(\alpha_0 a) j_{2m+\nu}(\alpha_0 a). \tag{25}$$

Since $k_0 = (\alpha^2 + \beta_0^2)^{1/2}$, and $j_n(\sigma) \sim O(\sigma^{-1})$ as $\sigma \to \infty$ it can be seen that the integrand in the definition of $K_{2m+\nu,2n+\nu}$ decays like $O(1/\alpha^3)$ as $\alpha \to \infty$. This rate of decay can be increased by adding and subtracting the leading order behaviour to the integrand, and using a result in [20, §6.574.2] to explicitly calculate the leading order contribution. There is one exception where this cannot be applied, when $m = n = \nu = 0$. For practical purposes this accelerated convergence is not necessary as accurate computations of (25) are numerically inexpensive. The computation of (25) involves principal-value integrals which are arranged as

$$\fint_0^{\infty} f(t)\, dt = \int_0^{t_0} \{f(t) + f(2t_0 - t)\}\, dt + \int_{2t_0}^{\infty} f(t)\, dt$$

for an integrand $f(t)$ which has a simple pole at $t = t_0$. Spherical Bessel functions are computed using a Fortran routine, [21][1].

Using (16) in (13) with (10) gives

$$T = 1 - \mathrm{i}\mu \sum_{n=0}^{\infty} a_n j_n(\alpha_0 a) = 1 - \mathrm{i}\mu \sum_{n=0}^{\infty} \{a_{2n} j_{2n}(\alpha_0 a) + a_{2n+1} j_{2n+1}(\alpha_0 a)\} \tag{26}$$

whilst

$$R = -\mathrm{i}\mu \sum_{n=0}^{\infty} a_n j_n(-\alpha_0 a) = -\mathrm{i}\mu \sum_{n=0}^{\infty} \{a_{2n} j_{2n}(\alpha_0 a) - a_{2n+1} j_{2n+1}(\alpha_0 a)\}. \tag{27}$$

[1] `http://fresco.org.uk/programs/barnett/SBESJY.FOR`

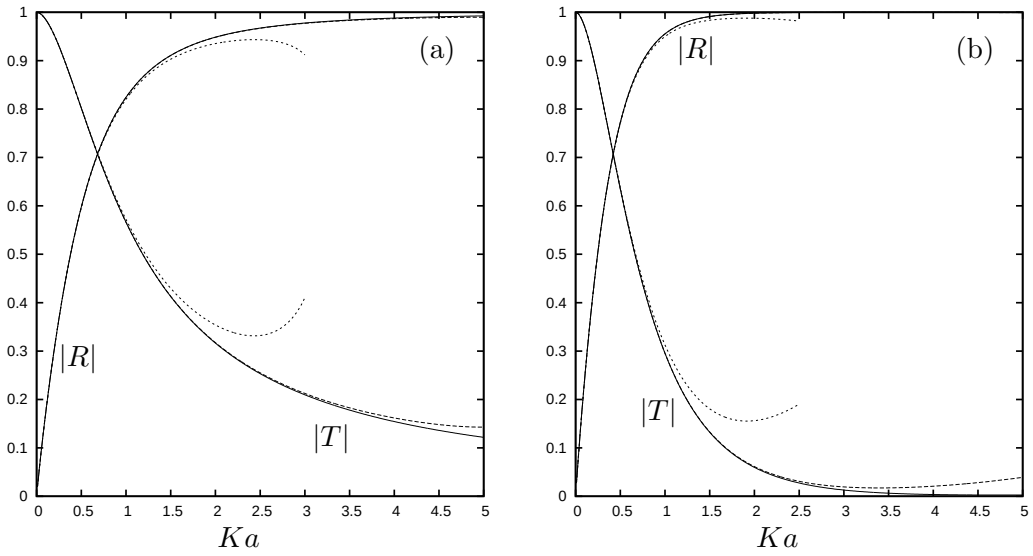


Figure 1: Modulus of the reflected wave amplitude as a function of $Ka = \omega^2 a/g$ for (a) normal incidence ($\theta_0 = 0°$) and (b) oblique incidence ($\theta = 45°$). Solid curve shows results for $N \geq 2$; dashed and dotted curves for $N = 1$, $N = 0$ approximations.

### *2.2. Approximation and results*

In order to compute numerical results we truncate the infinite system of equations (23) at $n, m = N$.

Choosing a truncation size of $N = 0$ constitutes a one-term approximation to the solution to the integral equations in which the variation in $\phi$ across the plate is assumed to be a constant. We may expect such an approximation to be valid when the $x$-component of the incident wavelength, $2\pi/\alpha_0$, is much larger than $2a$, the length of the plate, or $Ka\cos\theta_0 \ll \pi$. By extension of this hypothesis we expect larger values of $N$ to be needed in order to accurately resolve the scattering problem as the frequency of motion increases.

Figures 1(a),(b) show $|R|$ and $|T|$ against $Ka$ for incident wave angles of $\theta_0 = 0$ and $\theta_0 = 45°$ for $N = 0, 1, 2$. It can be seen that the $N = 0$ approximation performs well over a range of low frequencies, where the variation of $|R|$ and $|T|$ is at its greatest. The three-term ($N = 2$) approximation resolves the scattering amplitudes for $Ka < 5$ to an accuracy sufficient for any practical purpose being indistinguishable from results with higher values of $N$ over the range of frequencies shown.

In order to compare results from our method with existing results we have also computed reflection and transmission coefficients (as well as heave forces and roll moments) for water of finite depth, $h$. The changes to the method are minimal, requiring the denominator $k_0 - K$ in (25) to be replaced by $k_0 \tanh k_0 h - K$ and the definition of $\mu = K^2/\alpha_0$ to be replaced by $\mu =$

$\kappa^2 K/(\alpha_0(\kappa^2 h - K^2 h + K))$ where $\kappa$ satisfies the usual dispersion relation $K = \kappa \tanh \kappa h$. With $a/h = 1$ and $\theta_0 = 45^\circ$ we have reproduced exactly the figures shown in Table 2 of [6].

In passing, we remark that in, contrast to [6] and any method based on separation solutions, the present method avoids having to calculate the imaginary roots of the dispersion relation.

## 3. Three-dimensional scattering of waves by a finite dock

The problem is as stated previously apart from now the plate is no longer infinitely long but occupies a simply connected region $(x, y) \in \mathcal{D}$ in the surface $z = 0$. Special attention will eventually be paid to the case of a rectangular dock, where $\mathcal{D} = \{-a < x < a, -b < y < b\}$ although such restrictions are not needed initially.

The governing equations for $\Phi(x, y, z)$ are represented by (1)–(3), the incident wave potential is given by (4) and the zero-velocity condition on the plate is

$$\Phi_z = 0, \qquad (x, y) \in \mathcal{D}. \tag{28}$$

It is useful to introduce polar coordinates, $x = r\cos\theta$, $y = r\sin\theta$, into this problem. Then the radiation condition in three-dimensional scattering problems require that

$$\Phi(x, y, z) - \Phi_{inc}(x, y, z) \sim \sqrt{\frac{2}{\pi K r}} \mathrm{e}^{\mathrm{i}Kr - \mathrm{i}\pi/4} A(\theta; \theta_0) \mathrm{e}^{Kz} \quad Kr \to \infty \tag{29}$$

where $A(\theta; \theta_0)$ is the unknown complex diffraction coefficient measuring the complex wave amplitude in the direction $\theta$ for an incident wave in the direction $\theta_0$.

We define a double Fourier transform in $x$ and $y$ of the scattered part of the potential with

$$\overline{\Phi}(\alpha, \beta, z) = \int_{-\infty}^{\infty} \int_{-\infty}^{\infty} (\Phi(x, y, z) - \Phi_{inc}(x, y, z)) \mathrm{e}^{-\mathrm{i}\alpha x} \mathrm{e}^{-\mathrm{i}\beta y} \, dx \, dy. \tag{30}$$

Then it follows, taking transforms of (1), (3) that

$$\left( \frac{d^2}{dz^2} - k^2 \right) \overline{\Phi}(\alpha, \beta, z) = 0, \qquad z < 0 \tag{31}$$

where $k^2 = \alpha^2 + \beta^2$ and $\overline{\Phi}(\alpha, \beta, z) \to 0$ as $z \to -\infty$, whilst

$$\left( \frac{d}{dz} - K \right) \overline{\Phi}(\alpha, \beta, 0) = -K \overline{P}(\alpha, \beta) \tag{32}$$

where

$$\overline{P}(\alpha, \beta) = \iint_{\mathcal{D}} \Phi(x, y, 0) \mathrm{e}^{-\mathrm{i}\alpha x} \mathrm{e}^{-\mathrm{i}\beta y} \, dx \, dy \tag{33}$$

after the free surface condition (2) has been used for values of $(x, y) \notin \mathcal{D}$ and the condition (28) has been used for $(x, y) \in \mathcal{D}$. It follows that

$$\overline{\Phi}(\alpha, \beta, z) = \frac{K \overline{P}(\alpha, \beta)}{K - k} \mathrm{e}^{kz} \tag{34}$$

and taking inverse transforms results in

$$\Phi(x,y,z) = \Phi_{inc}(x,y,z) + \frac{K}{4\pi^2}\int_{-\infty}^{\infty}\int_{-\infty}^{\infty}\frac{\mathrm{e}^{kz}\mathrm{e}^{\mathrm{i}\alpha x}\mathrm{e}^{\mathrm{i}\beta y}}{K-k}\overline{P}(\alpha,\beta)\,d\alpha\,d\beta. \tag{35}$$

The integrand is singular along the circle $k \equiv \sqrt{\alpha^2+\beta^2} = K \equiv \sqrt{\alpha_0^2+\beta_0^2}$ in the $(\alpha,\beta)$-plane. It helps to make a change of variable, $\alpha = k\cos\psi$, $\beta = k\sin\psi$ so that (35) may be written

$$\Phi(x,y,z) = \Phi_{inc}(x,y,z) + \frac{K}{4\pi^2}\int_{0}^{2\pi}\int_{0}^{\infty}\frac{\mathrm{e}^{kz}\mathrm{e}^{\mathrm{i}kr\cos(\theta-\psi)}}{K-k}\overline{P}(k\cos\psi,k\sin\psi)\,kdk\,d\psi \tag{36}$$

and it is clear from what follows that the contour of integration in the $k$-plane must pass below the pole at $k=K$ on the axis of integration in order that scattered waves be outgoing at infinity.

We consider the limit $Kr\to\infty$ in the above, first collecting the contribution from the pole at $k=K$ in the $k$-integral and then using the method of stationary phase in the $\psi$-integral to obtain the dominant radiated wave contribution from the integral in (36). Lighthill [22] gives a formal account of this procedure, which is most easily justified by including a small imaginary part to the frequency $\omega$ so as to shift poles off real axes of integration.

Thus, the asymptotic behaviour for large $Kr$ of the integral in (36) may be equated to

$$\frac{-\mathrm{i}K^2}{2\pi}\mathrm{e}^{\mathrm{i}Kr-\mathrm{i}\pi/4}\sqrt{\frac{2\pi}{Kr}}\overline{P}(K\cos\theta,K\sin\theta)\mathrm{e}^{Kz}. \tag{37}$$

Comparing (37) with (29) via (35) gives

$$A(\theta;\theta_0) = \frac{-\mathrm{i}K^2}{2}\overline{P}(K\cos\theta,K\sin\theta) \tag{38}$$

and $\overline{P}$ is still an unknown function, having implicit dependence upon $\theta_0$. Returning to (35) and setting $z=0$ results in

$$\Phi(x,y,0) + (\mathcal{K}\Phi)(x,y) = \mathrm{e}^{\mathrm{i}\alpha_0 x}\mathrm{e}^{\mathrm{i}\beta_0 y} \tag{39}$$

where

$$(\mathcal{K}\Phi)(x,y) \equiv \frac{K}{4\pi^2}\int_{-\infty}^{\infty}\int_{-\infty}^{\infty}\frac{\mathrm{e}^{\mathrm{i}\alpha x}\mathrm{e}^{\mathrm{i}\beta y}}{k-K}\iint_{\mathcal{D}}\Phi(x',y',0)\mathrm{e}^{-\mathrm{i}\alpha x'}\mathrm{e}^{-\mathrm{i}\beta y'}\,dx'\,dy'\,d\alpha\,d\beta \tag{40}$$

after reinstating the definition of $\overline{P}$ from (33). Thus (39) acts as a second-kind integral equation for $\Phi(x,y,0)$ when $(x,y)\in\mathcal{D}$. For $(x,y)\notin\mathcal{D}$ it serves as a representation of $\Phi$ on the surface (and hence related to the free surface elevation) in terms of values of $\Phi$ on $\mathcal{D}$.

### *3.1. Solution for a rectangular dock*

The plate is defined by $\mathcal{D} = \{-a<x<a, -b<y<b\}$. We naturally extend the method used for the two-dimensional problem of §2 by first writing

$$\Phi(x,y,0) = \sum_{n=0}^{\infty}\sum_{m=0}^{\infty}a_{n,m}p_n(x/a)p_m(y/b) \tag{41}$$

where $p_n(t)$ are, as before, defined in (17). Substituting (41) in (39), multiplying by $p_p^*(x/a)p_q^*(y/b)$ and integrating over $\mathcal{D}$ results in the infinite system equations for coefficients $a_{n,m}$:

$$\frac{a_{p,q}}{4(2p+1)(2q+1)} + \sum_{n=0}^{\infty}\sum_{m=0}^{\infty} a_{n,m}K_{p,q,n,m} = j_p(\alpha_0 a)j_q(\beta_0 b), \qquad p,q = 0,1,2,\ldots \tag{42}$$

where

$$K_{p,q,n,m} = \frac{Kab}{4\pi^2}\int_{-\infty}^{\infty}\int_{-\infty}^{\infty} \frac{j_p(\alpha a)j_q(\beta b)j_n(\alpha a)j_m(\beta b)}{k-K}\,d\alpha\,d\beta \tag{43}$$

in terms of spherical Bessel functions, using (18).

Using symmetry properties of $j_n$ we note that $K_{p,q,n,m} = 0$ if either $n+p$ or $m+q$ is odd and this implies a decoupling of (42) into separate uncoupled systems for the four sets of coefficients $a_{2n,2m}$, $a_{2n+1,2m}$, $a_{2n,2m+1}$ and $a_{2n+1,2m+1}$, thus

$$\frac{a_{2p+\nu,2q+\mu}}{4(4p+1+2\nu)(4q+1+2\mu)} + \sum_{n=0}^{\infty}\sum_{m=0}^{\infty} a_{2n+\nu,2m+\mu}K_{2p+\nu,2q+\mu,2n+\nu,2m+\mu} = j_{2p+\nu}(\alpha_0 a)j_{2q+\mu}(\beta_0 b), \tag{44}$$

for $p,q = 0,1,2,\ldots$ and for $\nu,\mu = 0,1$ where

$$K_{2p+\nu,2q+\mu,2n+\nu,2m+\mu} = \frac{Kab}{\pi^2}\int_0^{\infty}\int_0^{\infty} \frac{j_{2p+\nu}(\alpha a)j_{2q+\mu}(\beta b)j_{2n+\nu}(\alpha a)j_{2m+\mu}(\beta b)}{k-K}\,d\alpha\,d\beta. \tag{45}$$

By first expressing this in polar form with $\alpha = k\cos\psi$, $\beta = k\sin\psi$ and using the fact that the contour in $k$ has been chosen to run under the pole at $k = K$ we can indent around the pole to extract the imaginary contribution to this integral and leave a real principal-value integral behind which decays like $O(1/k^4)$. Specifically,

$$\begin{aligned} K_{2p+\nu,2q+\mu,2n+\nu,2m+\mu} = & \\ & \frac{\mathrm{i}K^2ab}{\pi}\int_0^{\pi/2} j_{2p+\nu}(Ka\cos\psi)j_{2q+\mu}(Kb\sin\psi)j_{2n+\nu}(Ka\cos\psi)j_{2m+\mu}(Kb\sin\psi)\,d\psi \\ & + \frac{Kab}{\pi^2}\int_0^{\pi/2}\!\!\!\!\!\!\int_0^{\infty} \frac{j_{2p+\nu}(\alpha a)j_{2q+\mu}(\beta b)j_{2n+\nu}(\alpha a)j_{2q+\mu}(\beta b)}{k-K}k\,dk\,d\psi. \end{aligned} \tag{46}$$

It seems there is no further analytic simplification that can be made and the integrals must be approximated numerically.

Once the coefficients $a_{n,m}$ are found from (44) then the diffraction coefficient is readily given in terms of these coefficients after insertion of (41) in (38) with (33) to give

$$\begin{aligned} A(\theta;\theta_0) &= \frac{-\mathrm{i}K^2ab}{2}\sum_{n=0}^{\infty}\sum_{m=0}^{\infty} a_{n,m}j_n(Ka\cos\theta)j_m(Kb\sin\theta) \\ &\equiv \frac{-\mathrm{i}K^2ab}{2}\sum_{\nu,\mu=0,1}\sum_{n=0}^{\infty}\sum_{m=0}^{\infty} a_{2n+\nu,2m+\mu}j_{2n+\nu}(Ka\cos\theta)j_{2m+\mu}(Kb\sin\theta). \end{aligned} \tag{47}$$

The free surface elevation, normalised by the incident wave height, is $\Phi(x,y,0)$.

*3.2. Solution for a parallelogram-shaped dock*

The numerical method described above for a rectangular dock can be easily adapted to consider scattering by other shapes of dock which are defined by a linear map of a square. This is because a linear map preserves the separable nature and structure of the complex exponentials embedded in the integral equations (39).

Linear mappings of the square include a rectangle (which has already been considered), a rotation (which is equivalent to a rotation of the incident wave) and a parallelogram. Thus we consider here a parallelogram-shaped dock defined by $\mathcal{D} = \{-a + \lambda y < x < a + \lambda y, -b < y < b\}$ for some real parameter $\lambda$. We write

$$\Phi(x, y, 0) = \sum_{n=0}^{\infty} \sum_{m=0}^{\infty} a_{n,m} p_n((x - \lambda y)/a) p_m(y/b) \tag{48}$$

for $(x, y) \in \mathcal{D}$. Consequently, application of the solution method in conjunction with the linear map $t = (x - \lambda y)/a$, $u = y/b$, readily results in the system

$$\frac{a_{p,q}}{4(2p+1)(2q+1)} + \sum_{n=0}^{\infty} \sum_{m=0}^{\infty} a_{n,m} K_{p,q,n,m} = j_p(\alpha_0 a) j_q(\beta_0 b + \lambda \alpha_0 b), \qquad p, q = 0, 1, 2, \ldots \tag{49}$$

where, now,

$$K_{p,q,n,m} = \frac{Kab}{4\pi^2} \int_{-\infty}^{\infty} \int_{-\infty}^{\infty} \frac{j_p(\alpha a) j_q(\beta b + \lambda \alpha b) j_n(\alpha a) j_m(\beta b + \lambda \alpha b)}{k - K} \, d\alpha \, d\beta. \tag{50}$$

Now we can see (most easily after converting the integration to polar coordinates) that $K_{p,q,n,m} = 0$ if $p + q + n + m$ is odd, and

$$K_{p,q,n,m} = \frac{Kab}{2\pi^2} \int_0^{\pi} \int_0^{\infty} \frac{j_p(\alpha a) j_q(\beta b + \lambda \alpha b) j_n(\alpha a) j_m(\beta b + \lambda \alpha b)}{k - K} \, k dk \, d\psi \tag{51}$$

(with $\alpha = k \cos\psi$, $\beta = k \sin\psi$ as usual) if $p + q + n + m$ is even. This allows the general system of equations (49) to be decoupled into two systems, one for $a_{n,m}$ when $n + m$ is even applied over values of $p+q$ even and one for $a_{n,m}$ when $n+m$ odd applied over $p+q$ odd. This decoupling reflects the rotational symmetry of the parallelogram and aids the efficiency of the numerical solution.

*3.3. Other dock shapes*

There are more direct methods for dealing with circles, such as using Hankel transforms in a radial direction and Fourier series in the azimuthal direction, so these will not be considered here.

For arbitrary domains $\mathcal{D}$ it is possible to fit a mesh to $\mathcal{D}$ and expand $\Phi$ over the mesh using a finite-element basis. The Galerkin method can still be employed and one would want to choose a mesh and basis such that integrals over spatial variables can be done exactly. Of course, this would lead to a large matrix system to invert and all the advantages of the method described so far are lost. In this respect it is probably easiest to return to a Green's function formulation of the problem for arbitrary domains, in a manner similar to [12].

*3.4. Forces, moments and radiated waves*

The heave exciting force, $X_h$, and the pitch and roll exciting moments, $X_p$, $X_r$, about the $y$ and $x$ axes respectively, on the plate due to incident waves are given by

$$X_{h,p,r} = -\mathrm{i}\omega\rho \iint_{\mathcal{D}} \Phi(x,y,0)\{1,x,y\}\,dxdy. \tag{52}$$

For a rectangular plate, we use the fact that $P_0(x) = 1$ and $P_1(x) = x$ in conjunction with the expansion for $\Phi(x,y,0)$ in (41) to give

$$X_{h,p,r} = -\mathrm{i}\omega ab\rho\{a_{0,0}, \tfrac{1}{3}\mathrm{i}aa_{1,0}, \tfrac{1}{3}\mathrm{i}ba_{0,1}\}. \tag{53}$$

It is also straightforward to develop solutions to a variant of the scattering problem described above in which the plate radiates waves due to forced motion in heave, roll or pitch in the absence of incident waves. Since forced roll and pitch are related for a rectangular plate, we consider just heave and roll in what follows. We start with potentials $\Phi^{(h,p)}(x,y,z)$ satisfying Laplace's equation, the free surface condition, and deep water condition, (1)–(3). The revisions to the formulation of integral equations for $\Phi^{(h,p)}(x,y,0)$ include, obviously, removing the incident wave and replacing (28) with the forced-motion condition

$$\frac{\partial\Phi^{(h,p)}}{\partial z} = \{1,x\}, \qquad \text{on } z=0,\ (x,y)\in\mathcal{D}. \tag{54}$$

The incident wave potentials are also removed from the definition (30) of the Fourier transform.

Following the methods described for the scattering problem earlier in this section, the transform solution incorporates this forcing as

$$\overline{\Phi}^{(h,p)}(\alpha,\beta,z) = \frac{K\overline{P}^{(h,p)}(\alpha,\beta) - \overline{F}^{(h,p)}(\alpha,\beta)}{K-k}\mathrm{e}^{kz} \tag{55}$$

where

$$\begin{aligned}\overline{F}^{(h,p)}(\alpha,\beta) &= \iint_{\mathcal{D}} \{1,x\}\mathrm{e}^{-\mathrm{i}\alpha x}\mathrm{e}^{-\mathrm{i}\beta y}\,dxdy \\ &\equiv 4ab\{j_0(\alpha a)j_0(\beta b), -\mathrm{i}aj_1(\alpha a)j_0(\beta b)\}\end{aligned} \tag{56}$$

and $\overline{P}^{(h,p)}$ is defined by (33) but with $\Phi$ replaced by $\Phi^{(h,p)}$. The final calculations in (56) above have been made using $P_0(x) = 1$, $P_1(x) = x$ and the relation (18). Taking inverse transforms and setting $z = 0$ results in the integral equation

$$\Phi^{(h,p)}(x,y,0) + \left(\mathcal{K}\Phi^{(h,p)}\right)(x,y) = F^{(h,p)}(x,y) \tag{57}$$

for $(x,y) \in \mathcal{D}$ where the integral operator $\mathcal{K}$ is identical to (40) used in the scattering problem. The difference between (39) and (57) is that the incident wave forcing of the integral equation has been replaced by

$$F^{(h,p)}(x,y) = \frac{1}{4\pi^2}\int_{-\infty}^{\infty}\int_{-\infty}^{\infty} \frac{\overline{F}^{(h,p)}(\alpha,\beta)}{k-K} \mathrm{e}^{\mathrm{i}\alpha x}\mathrm{e}^{\mathrm{i}\beta y}\, d\alpha d\beta. \tag{58}$$

Following an application of the Galerkin method to reduce the integral equations to infinite systems of equations, in which we write

$$\Phi^{(h,p)}(x,y,0) = \sum_{n=0}^{\infty}\sum_{m=0}^{\infty} a_{n,m}^{(h,p)} p_n(x/a) p_m(y/b) \tag{59}$$

we find that the expansion coefficients are determined from

$$\frac{a_{2p,2q}^{(h)}}{4(4p+1)(4q+1)} + \sum_{n=0}^{\infty}\sum_{m=0}^{\infty} a_{2n,2m}^{(h)} K_{2p,2q,2n,2m} = \frac{4}{K} K_{2p,2q,0,0}, \tag{60}$$

and

$$\frac{a_{2p+1,2q}^{(p)}}{4(4p+3)(4q+1)} + \sum_{n=0}^{\infty}\sum_{m=0}^{\infty} a_{2n+1,2m}^{(p)} K_{2p+1,2q,2n+1,2m} = \frac{-4\mathrm{i}a}{K} K_{2p+1,2q,1,0}, \tag{61}$$

each for $p,q = 0,1,2,\ldots$. All other components of the coefficients other than those determined by the above systems of equations are zero. For example, heave motion of a rectangular plate generates a fluid motion which is symmetric in both planes $x=0$ and $y=0$ and hence all but the coefficients $a_{2n,2m}^{(h)}$ must be zero. We also note that, from a computational perspective, the solutions to the two sets of equations in (60) and (61) are essentially 'free' once the scattering problem has been computed since the most expensive parts of the calculation (the formulation and inverse of the matrix on the left-hand side of the equations) are common to both scattering and radiation problems.

Quantities of interest associated with the radiation problem typically involve the added mass and radiation damping coefficients, being associated with the real and imaginary components of the complex forces and moments on the plate induced by its own motion. For example, these quantites are required for calculating the response of a constrained or freely-floating plate in the surface. For the problems outlined above these are readily found, using formulae (52), (53) applied to heave and roll potentials, to be given by

$$\begin{aligned} -\mathrm{i}\omega A_{hh} + B_{hh} &= -\mathrm{i}\omega\rho a b a_{0,0}^{(h)} \\ -\mathrm{i}\omega A_{pp} + B_{pp} &= \omega\rho\tfrac{1}{3}a^2 b a_{1,0}^{(p)} \end{aligned} \tag{62}$$

where $A_{hh}$ refers to the heave added mass due to forced heave motion etc. Note there is no heave induced added mass or damping due to roll motion and vice versa by symmetry.

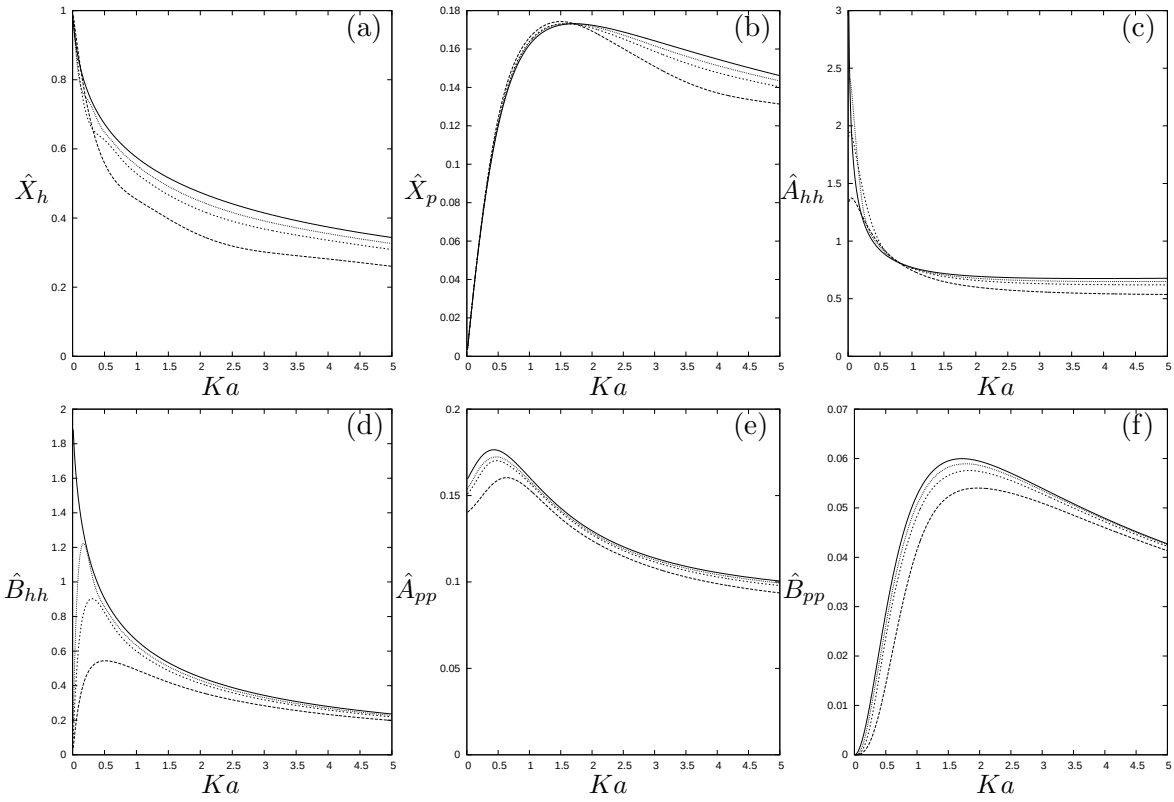


Figure 2: Exciting and radiation force components against frequency parameter $Ka$ on a rectangular dock with $b/a = 2$ (long-dashed) $b/a = 5$ (short-dashed) $b/a = 10$ (dotted) and the comparison with results from two-dimensional dock (solid): (a) heave exciting force and (b) roll exciting moment due to $\theta = 0$ incident waves; (c) Heave added mass and (d) heave radiation damping due to heave motion; (e) roll added inertia and (f) roll radiation damping due to roll motion. Series truncated to five terms.

*3.5. Results*

For the heave exciting forces and moments we define the non-dimensional quantities

$$\hat{X}_h = \frac{X_h}{4\rho ab\omega}, \qquad \hat{X}_p = \frac{X_p}{4\rho a^2 b\omega}, \qquad \hat{X}_r = \frac{X_r}{4\rho ab^2\omega}, \tag{63}$$

and for the radiated waves, we define non-dimensional quantities with

$$\hat{A}_{hh} = \frac{A_{hh}}{4\rho a^2 b}, \qquad \hat{B}_{hh} = \frac{B_{hh}}{4\rho\omega a^2 b}, \qquad \text{and} \qquad \hat{A}_{pp} = \frac{A_{pp}}{4\rho a^4 b}, \qquad \hat{B}_{pp} = \frac{B_{pp}}{4\rho\omega a^4 b}. \tag{64}$$

In a simplified but similar fashion to §3.4 hydrodynamic forces can be calculated for the two-dimensional plate considered in the previous section. This allows us to compare results for retangular plates of finite length and width from §3.4 with the corresponding two-dimensional results for infinitely-long plates of the same finite width. Thus, in figures 2(a)–(f) the hydrodynamic force coefficients have been plotted for plates of length-to-width ratios $b/a$ of 2, 5 and 10 alongside the corresponding two-dimensional results for an infinitely-long plate. Both sets of results have been non-dimensional per unit length of the plate to allow this comparison to be made. We see quite clearly in figures 2(a)–(f) that as $b/a$ increases the curves approach the two-dimensional results. Indeed, we can infer that, for most of the hydrodynamic force coefficients, the three-dimensional forces are similar to the two-dimensional counterparts for most values of frequency. There are some quite interesting differences in behaviour at low and high frequencies. For example, from figure 2(d) $\hat{B}_{hh}$ has a non-zero limit as $Ka \to 0$ for the infinitely-long two-dimensional plate but tends zero as $Ka \to 0$ for a finite rectangular plate. Also, in constrast to all other coefficients, figure 2(b) shows the low frequency agreement between $\hat{X}_p$ for finite and infinite length plates to be remarkably good, but the agreement is less good for higher $Ka$. These effects are not understood, but appear not to be a result of poor numerical resolution.

In figure 3(a,b) we illustrate examples of shaded plots of maximum free surface amplitudes. Here, $a/b = 1$ and the axes are scaled so that the plate (shaded black) occupies the square $|x/a| < 1$, $|y/a| < 1$. Plots are shown for incident waves propagating in the directions $\theta = 0$ and $\theta = 45°$. There is clear graphical evidence of reflected plane waves from the plane edges of the dock and a shadow zone downwave of the dock. The free surfaces were calculated here using $4 \times 4$ terms in the expansion of $\Phi(x, y, 0)$ under the plate, with no difference being noted when more terms are taken in the series.

Results for a parallelogram-shaped dock are illustrated by the two free-surface plots in figures 4(a,b). The first is the maximum amplitude and the second is a snapshot in time of the surface. The waves are propagating in the positive $x$-direction with $Ka = 4$ and $a/b = 1$, $\lambda = 1$ so that the sides of the parallelogram are titled at 45° to top and the bottom edges. Computations are

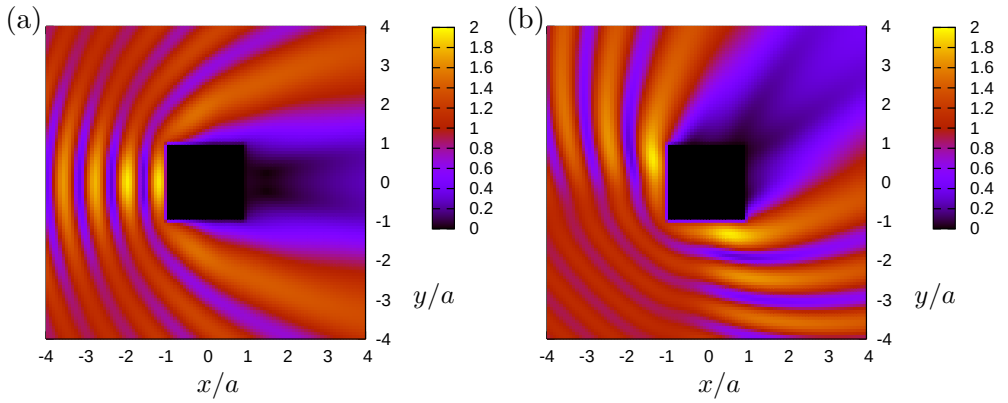


Figure 3: Modulus the total wave field $|\Phi(x, y)|$ for an incident wave of unit amplitude with $Ka = 4$, $\theta_0 = 0°$ in (a) and $\theta_0 = 45°$ in (b) for a dock with $a = b$. The dock is shaded black.

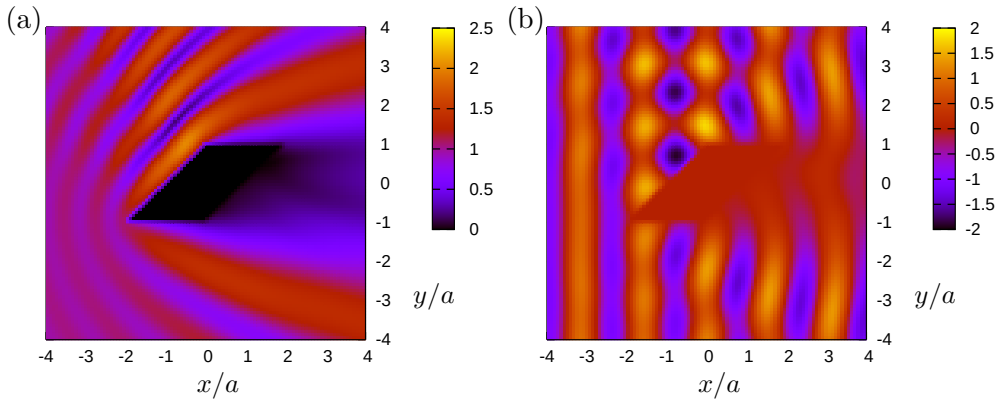


Figure 4: (a) Maximum amplitude, $|\Phi(x, y, 0)|$, and (b) snapshot in time, $\Re\{\Phi(x, y, 0)\}$, of the total wave field for an incident wave of unit amplitude with $Ka = 4$, $a/b = 1$, $\lambda = 1$ and $\theta_0 = 0°$. The dock is shaded black in (a).

performed using a decoupling of (49) into odd and even systems with (51). Again we see that for this relatively high-frequency incident wave there is a clear signal of a reflected wave propagating in the positive $y$-direction from the leading edge of the dock and a shadow region upwave of the dock.

### *3.6. Freely-floating plates*

For a freely-floating rectangular plate, horizontal dimensions $2a \times 2b$, thickness $h$ and density $\rho_s < \rho$, a straightforward application of Newton's law (e.g. [23, §6.19]) allows the heave excursion and roll angle per unit incident wave amplitude to be expressed as $\Re\{z\mathrm{e}^{-\mathrm{i}\omega t}\}$, $\Re\{\theta\mathrm{e}^{-\mathrm{i}\omega t}\}$ where

$$z = \frac{\mathrm{i}gX_h}{\omega^2(B_{hh} - \mathrm{i}\omega(M + A_{hh} - C_h/\omega^2))}$$

and

$$\theta = \frac{\mathrm{i}gaX_p}{\omega^2(B_{pp} - \mathrm{i}\omega(I + A_{pp} - C_p/\omega^2))}.$$

In the above $M = 4\rho_s abh$, $I = \frac{1}{6}\rho_s ah(4a^2 + h^2)$, $C_h = 4\rho abg$ and $C_p = \frac{2}{3}\rho g a^3$. For a plate under oblique incidence, there is a corresponding independent equation expressing the pitch angle. No computations of these quantities are shown here.

## 4. The 'ice fishing problem'

A rigid lid along $z = 0$ covers a fluid occupying $z < 0$ apart from over the finite-width channel $|x| < a$, $-\infty < y < \infty$ where there is a free surface. That is, the plate is taken to occupy the complementary region of $z = 0$ to that considered in §2. This problem is often referred to (e.g. [14]) as the 'ice fishing problem'. Assuming a $\beta_0$ wavenumber component in the $y$-direction we find, using a straightforward application of methods outlined previously the homogeneous integral equation

$$\phi(x,0) - \frac{K}{2\pi}\int_{-\infty}^{\infty}\frac{\mathrm{e}^{\mathrm{i}\alpha x}}{k_0}\int_{-a}^{a}\phi(x',0)\mathrm{e}^{-\mathrm{i}\alpha x'}\,dx'd\alpha = 0, \qquad |x| < a \tag{65}$$

where $k_0 = \sqrt{\alpha^2 + \beta_0^2}$, which determines the eigenfrequencies, related to $K$, of sloshing modes in the free surface. Using expansions in terms of Legendre polynomials as before leads to the two decoupled infinite systems of equations

$$\frac{\pi a_{2m+\nu}}{2Ka(4m+2\nu+1)} - \sum_{n=1-\nu}^{\infty} a_{2n+\nu}K_{2m+\nu,2n+\nu} = 0, \qquad m \geq 1-\nu, \tag{66}$$

where

$$K_{2m+\nu,2n+\nu} = \int_0^{\infty}\frac{j_{2m+\nu}(t)j_{2n+\nu}(t)}{\sqrt{t^2+(\beta_0 a)^2}}dt \tag{67}$$

where $\nu = 0$ for symmetric modes and $\nu = 1$ for antisymmetric modes. There is a small change required in the application of the expansion, being the omission of the $n = 0$ term on account of it violating mass conservation. Consequently the starting value of $n$ in the infinite series in (66) is $n = 1$ for $\nu = 0$ and $n = 0$ for $\nu = 1$.

In other words the values of $\pi/Ka$ for the sloshing modes are given by the eigenvalues of the infinite symmetric matrices with entries

$$I^{(\nu)}_{m,n} = 2(4m+2\nu+1)^{1/2}(4n+2\nu+1)^{1/2}\int_0^{\infty}\frac{j_{2m+\nu}(t)j_{2n+\nu}(t)}{\sqrt{t^2+(\beta_0 a)^2}}dt \tag{68}$$

for $m, n \geq 1-\nu$.

In the particular case of two-dimensional sloshing modes in which the denominator of (68) reduces simply to $t$ further analytic progress can be made. We first substitute Bessel functions in place of spherical Bessel functions using (20) so that (68) becomes

$$I^{(\nu)}_{n,m} = \pi(4m+2\nu+1)^{1/2}(4n+2\nu+1)^{1/2}\int_0^{\infty}\frac{J_{2m+\nu+1/2}(t)J_{2n+\nu+1/2}(t)}{t^2}dt. \tag{69}$$

and the integrals above may be evaluated directly using [20, §6.574.2] resulting in

$$I_{n,m}^{(\nu)} = \frac{(-1)^{n+m}(4m+2\nu+1)^{1/2}(4n+2\nu+1)^{1/2}}{(m+n+\nu)(m+n+\nu+1)(1-4(n-m)^2)}. \tag{70}$$

These expressions are identical to those given by Davis [15], modulo a factor of $(-1)^{n+m}$ which does not affect the eigenvalues. This is not surprising as we have, in effect, used the same approach as [15] in formulating integral equations for the unknown potential across the hole $|x| < a$. [15] used a Green's function to formulate his integral equation with expansions of the unknown $\phi(x,0)$ in terms of Legendre polynomials. The derivation of the final result required more effort than in our approach.

There are no obvious results which allow similar analytic progress of the evaluation of integrals in (68) to be made when $\beta_0 \neq 0$.

A selection of results, computed in all cases, including when $\beta_0 = 0$, using (68), are given in table 1 for three different values of $\beta_0 a$. A matrix truncation size of 40 was used to ensure convergence of the eigenvalues to the five decimal places shown. It appears that the eigenvalues of the truncated infinite matrix are more sensitive to truncation than solutions to truncated infinite systems of equations encountered in earlier scattering problems. When $\beta_0 a = 0$, the values coincide with those computed in [15]. No effort has been made to replicate or extend the methods of [15] in considering the asymptotic forms for the eigenvalue distribution for $\beta_0 \neq 0$

The quasi two-dimensional problem of sloshing modes in an infinitely-long channel is readily extended to a finite rectangular fishing hole. Now it is found that the eigenvalues of infinite matrices with entries

$$\begin{aligned} I_{n,m,p,q}^{(\nu,\mu)} &= (4q+2\mu+1)^{1/2}(4p+2\nu+1)^{1/2}(4m+2\mu+1)^{1/2}(4n+2\nu+1)^{1/2} \\ &\quad \times \int_0^\infty \int_0^\infty \frac{j_{2p+\nu}(\alpha a) j_{2q+\mu}(\beta b) j_{2n+\nu}(\alpha a) j_{2m+\mu}(\beta b)}{\sqrt{\alpha^2+\beta^2}} d\alpha d\beta \end{aligned}$$

are $\pi^2/(4Kab)$ for $\nu, \mu = 0, 1$ corresponding to mode symmetry/antisymmetry in $x = 0$ and $y = 0$. The matrix entries are for $n, m, p, q \geq 0$ in all cases except where $\nu = \mu = 0$ where $n, m, p, q \geq 1$ is used on account of mass conservation considerations. For computational purposes truncated square matrices have been constructed from the elements $I_{n,m,p,q}^{(\nu,\mu)}$ by an appropriate indexing mechanism.

Again, there is no obvious way of simplifying the integrals in the above. The numerical integration is performed by the change of variables $\alpha = k\cos\psi$, $\beta = k\sin\psi$ used previously in this paper.

Table 2 shows the first ten eigenvalues, $Ka/\pi$, for the four different symmetry groupings corresponding to sloshing motions in a rectangular fishing hole with $a/b = \frac{1}{4}$. For example, $(Ka)_{sa}$

| | $\beta_0 a = 0$ | | $\beta_0 a = 1$ | | $\beta_0 a = 5$ | |
|---|---|---|---|---|---|---|
| $n$ | $(Ka)_s/\pi$ | $(Ka)_a/\pi$ | $(Ka)_s/\pi$ | $(Ka)_a/\pi$ | $(Ka)_s/\pi$ | $(Ka)_a/\pi$ |
| 1 | 1.09923 | 0.63856 | 1.16893 | 0.77919 | 2.02935 | 1.81400 |
| 2 | 2.10995 | 1.63143 | 2.14613 | 1.69086 | 2.73070 | 2.39096 |
| 3 | 3.11432 | 2.62923 | 3.13851 | 2.66574 | 3.56754 | 3.16489 |
| 4 | 4.11671 | 3.62815 | 4.13482 | 3.65434 | 4.46973 | 4.03456 |
| 5 | 5.11822 | 4.62752 | 5.13268 | 4.64788 | 5.40592 | 4.95248 |
| 6 | 6.11927 | 5.62710 | 6.13129 | 5.64375 | 6.36146 | 5.89686 |
| 7 | 7.12003 | 6.62680 | 7.13031 | 6.64087 | 7.32886 | 6.85696 |
| 8 | 8.12062 | 7.62658 | 8.12960 | 7.63876 | 8.30402 | 7.82706 |
| 9 | 9.12108 | 8.62641 | 9.12905 | 8.63714 | 9.28450 | 8.80387 |
| 10 | 10.1215 | 9.62627 | 10.1286 | 9.63586 | 10.2688 | 9.78539 |

Table 1: The first 10 values of $Ka$ for symmetric and antisymmetric sloshing motions for a fishing hole of width $2a$ in the two-dimensional problem for three different values of wave obliqueness, $\beta_0 a$. Columns 2 and 3 coincide with tabulated values in [15].

implies symmetry about $y = 0$ and antisymmetry about $x = 0$. Numerically the size of the truncated system has been increased until the values of $Ka/\pi$ shown have converged to the five decimal places shown. This has happened with truncation sizes of 16 in $n, m, p, q$ implying that the eigenvalues of a $256 \times 256$ matrix have been determined for each of the four symmetry groups. The distribution of eigenvalues are similar to those one would find when considering the wave equation with free wavenumber $K$ on a rectangular domain, $|x| < a$, $|y| < b$, with Neumann conditions on the domain boundaries.

It has been confirmed numerically that the first entries in columns 2 and 4 tend to the first two entries in columns 2 and 3 in table 1 as $a/b$ becomes larger. This is evidently on account of the first eigenmode becoming increasingly two-dimensional as the length of the hole is increased. As expected, interchanging $a$ and $b$ results in the same eigenvalues, whilst if $a/b = 1$ columns 3 and 4 are found to be identical.

With some further effort, calculations of eigenvalues for the fishing-hole problem for parallelogram-shaped holes could also be made.

| $n$ | $(Ka)_{ss}/\pi$ | $(Ka)_{sa}/\pi$ | $(Ka)_{as}/\pi$ | $(Ka)_{aa}/\pi$ |
|---|---|---|---|---|
| 1 | 1.17425 | 0.31519 | 0.66333 | 0.71834 |
| 2 | 1.29457 | 0.53873 | 0.78794 | 0.86744 |
| 3 | 1.44543 | 0.76652 | 0.95392 | 1.04597 |
| 4 | 1.61733 | 0.99960 | 1.14234 | 1.24235 |
| 5 | 1.80441 | 1.17912 | 1.34529 | 1.45075 |
| 6 | 2.00277 | 1.23706 | 1.55822 | 1.66380 |
| 7 | 2.15119 | 1.28582 | 1.64179 | 1.67025 |
| 8 | 2.20936 | 1.42109 | 1.70070 | 1.74353 |
| 9 | 2.22311 | 1.47803 | 1.77781 | 1.84912 |
| 10 | 2.31908 | 1.58089 | 1.79430 | 1.89156 |

Table 2: The first 10 values of $Ka$ for sloshing motions with symmetry/antisymmetry about $y = 0$ and $x = 0$ for a rectangular fishing hole with sides $2a$, $2b$ and $a/b = \frac{1}{4}$.

## 5. Conclusion and further work

In this paper we have applied Fourier transform methods to solve wave scattering and radiation problems associated with rigid plates, or docks, held fixed on the surface of a fluid. We first demonstrated the method in the simple setting of a two-dimensional problem, in which the dock is infinitely long in one direction and upon which waves are obliquely incident. The extension to the three-dimensional problem in which a finite two-dimensional dock is held fixed in the surface is treated similarly leading to a more complicated problem but of essentially the same structure as the simpler problem in a reduced dimension. In both cases, second kind integral equations are formulated and solved using a Galerkin method. Numerical results are shown to converge rapidly with increasing terms in the expansion and key properties such as diffracted wave ampltiudes and hydrodynamic forces readily expressed in terms of the numerical solutions.

In both this work and the earlier work of [7] it has been demonstrated that the application of transforms methods can lead to substantially simpler solution when compared to, for example, eigenfunction matching methods (e.g. [5]) or the application of Green's function (e.g. [10]). They are also equally applicable in finite or infinite depth with little modification required in the formulation or the numerical solution. However, they are restricted to a certain class of problems where boundaries of domain are aligned.

Flexible plates on the surface have been considered using an extension of the current approach and will be reported elsewhere. An extension to consider waves interaction with multiple plates,

connected by hinges through which power is extracted, is also being considered as a model of certain types of articulated pontoon-type wave energy converters.

A final extension to consider is that of a dock of finite width and semi-infinite length. Progress (not reported here) has been made in combining the solutions to the infinite two-dimensional dock problem in §2 with the finite dock problem in §3. However, the solution is not fully resolved, at least in terms of exactly how to implement an effective and efficient numerical method.

## References


[1] A.E. Heins. Water waves over a channel of finite depth with a dock. *American Journal of Mathematics,* **70**:730-748, 1948.

[2] K.O. Friedrichs & H. Lewy. The dock problem. *Comm. Applied Maths*, **1**:135-148, 1948.

[3] R.L. Holford. Short surface waves in the presence of a finite dock. I. *Proc. Camb. Phil. Soc.*, **60**:957-983, 1964.

[4] F.G. Leppington. On the scattering of short surface waves by a finite dock. *Proc. Camb. Phil. Soc.*, **64**:1109-1129, 1968.

[5] C.M. Linton & P. McIver. Handbook of Mathematical Techniques for Wave/Structure Interactions. *CRC Press: Southampton*, 2001.

[6] C.M. Linton. The finite dock problem. *Z. angew. Math. Phys.* **52**:640–656, 2002.

[7] R. Porter. Linearised water wave problems involving submerged horizontal plates. *Appl. Ocean Res.* **50**:91–109, 2015.

[8] P.A. Martin & S.G. Llewellyn Smith. Generation of internal gravity waves by an oscillating horizontal disc. *Proc. Roy. Soc. Lond. A* **467**(2136):3406–3423, 2011.

[9] R.V. Craster. Scattering by cracks beneath fluid-solid interfaces *J. Sound Vib.* **15**(2):343–372, 1998.

[10] R. Eatock-Taylor. Hydroelastic analysis of plates and some approximations *J. Eng. Maths.* **58**(1) 267–278.

[11] A.A. Dorfman. Water waves diffraction by a circular plate. *J Comp. Appl. Maths.* **110**:287–304, 1999.

[12] M.H. Meylan. Wave response of an ice floe of arbitrary geometry. *J. Geo. Res.: Oceans (1978-2012)* **107**(C1) 5-1–5-11, 2002.

[13] L.G. Bennetts & T.D. Williams. Wave scattering by ice floes and polynyas of arbitrary shape. *J. Fluid Mech.* **662** 5–35.

[14] V. Kozlov & N.G. Kuznetsov. The ice-fishing problem: the fundamental sloshing frequency versus geometry of holes. *Math. Meth. Appl. Sci.* **27**:289–312, 2004.

[15] A.M.J. Davis. Waves in the presence of an infinite dock with gap. *IMA J. Appl. Maths.* **6**(2):141–156, 1970.

[16] J.W. Miles. On the eigenvalue problem for fluid sloshing in a half-space *Z. angew. Math. Phys.* **21**:861–868, 1972.

[17] D.W. Fox & J.R. Kuttler. Sloshing frequencies. *Z. angew. Math. Phys.* **34**:668–696, 1983.

[18] N.M. Wigley. Asymptotic expansions at a corner of solutions of mixed boundary value problems. *J. Math. Mech.* **13**(4):549–576, 1964.

[19] M. Abramowitz & I. A. Stegun. Handbook of Mathematical Functions. New York: Dover, 1965.

[20] I.S. Gradshteyn & I.M. Ryzhik. Table of Integrals Series and Products. Academic Press, 1980.

[21] A.R. Barnett. The calculation of spherical Bessel and Coulomb functions. In *Computational Atomic Physics*, Ed. K. Bartschat. pp181–202, 1996.

[22] M.J. Lighthill. Studies on Magneto-Hydrodynamic Waves and other Anisotropic Wave Motions. *Phil. Trans. A.* **252**(1014):397–430, 1960.

[23] J.N. Newman Marine Hydrodynamics. The MIT Press, 1977.